Using MD Snapshots in ab Initio and DFT Calculations: OH Vibrations in the First Hydration Shell around Li + (aq)

ARTICLE *in* THE JOURNAL OF PHYSICAL CHEMISTRY A · JULY 2005

Impact Factor: 2.69 · DOI: 10.1021/jp047395j · Source: PubMed

3 AUTHORS:

Ljupco Pejov
Ss. Cyril and Methodius University
108 PUBLICATIONS **846** CITATIONS
SEE PROFILE

Daniel Spångberg
39 PUBLICATIONS **852** CITATIONS
SEE PROFILE

Kersti Hermansson
Uppsala University
203 PUBLICATIONS **4,684** CITATIONS
SEE PROFILE

Using MD Snapshots in ab Initio and DFT Calculations: OH Vibrations in the First Hydration Shell around Li^+(aq)

Ljupčo Pejov,[†] Daniel Spångberg,[‡] and Kersti Hermansson*[,‡]

Institute of Chemistry, Faculty of Science, "Sts. Cyril and Methodius University", P.O. Box 162, 1000 Skopje, Republic of Macedonia, and Materials Chemistry, The Ångström Laboratory, Uppsala University, Box 538, S-751 21 Uppsala, Sweden

Received: June 16, 2004; In Final Form: November 5, 2004

The average OH stretching vibrational frequency for the water molecules in the first hydration shell around a Li^+ ion in a dilute aqueous solution was calculated by a hybrid molecular dynamics + quantum-mechanical ("MD + QM") approach. Using geometry configurations from a series of snapshots from an MD simulation, the *anharmonic*, uncoupled OH stretching frequencies were calculated for 100 first-shell OH oscillators at the B3LYP and HF/6-31G(d,p) levels of theory, explicitly including the first shell and the relevant second shell water molecules into charge-embedded supermolecular QM calculations. Infrared intensity-weighting of the density-of-states (DOS) distributions by means of the squared dipole moment derivatives (which vary by a factor of 20 over the OH stretching frequency band at the B3LYP level), changes the downshift from approximately -205 to -275 cm^{-1} at the B3LYP level. Explicit inclusion of relevant third-shell water molecules in the supermolecular cluster leads to a further downshift by approximately -30 cm^{-1}. Our final estimated average downshift is approximately -305 cm^{-1}. The experimental value lies somewhere in the range between -290 and -420 cm^{-1}. Also, the absolute ν(OH) frequency is well reproduced in our calculations. "In-liquid" instantaneous correlation curves between ν(OH) and various typical H-bond strength parameters such as R(O···O), R(H···O), the intramolecular OH bond length, and the IR intensity are presented. Some of these correlations are robust and persist also for the rather distorted instantaneous geometries in the liquid; others are less so.

1. Introduction

Ion solvation is of central importance in solution chemistry.[1,2] Nevertheless it is generally difficult to produce unambiguous molecular-level solvation information, even regarding such fundamental quantities as, for example, the average number of solvent molecules residing in the first solvation shells around the ions. The present paper is not mainly concerned with solvation structure but with a related and equally difficult issue, namely how the solvent molecules in the solvation shells are themselves modified by the presence of the ions. Molecular properties which are sensitive to the surroundings of the molecule can be used, and are being used, as powerful structural probes. One such set of environmental-sensitive properties are the molecular vibrational frequencies (see, for example, refs 1−7).

The vibrational energy levels can be obtained *from experiment* using infrared (IR) and Raman spectroscopy and from theory by a number of techniques at different levels of sophistication. In practice, a main experimental obstacle in vibrational studies of ionic solutions is the difficulty to single out the spectral contributions originating from the ion-bound molecules from those originating from the bulk molecules. The "double-difference method" developed by Lindgren et al.[8−10] describes one way to circumvent this problem. Another experimental obstacle is the assignment of the correct vibrational mode to each of the various spectral peaks observed. Here the isotope-isolation technique[11−13] has been much used in the case of aqueous solutions: a small percentage of HDO molecules among a large number of surrounding H_2O (or D_2O) molecules makes the O−D (or O−H) oscillators of the HDO molecules behave as essentially *uncoupled from all other water vibrations*; this makes the experimental signal clearer, and the analysis of the vibrational pattern becomes more straightforward. Also the external influence on the intramolecular stretching vibrations becomes easier to interpret using this technique. Without the isotope-isolation technique, couplings may occur between intermolecular stretching vibrations and between stretching vibrations and the bending overtone, as well as between intra- and intermolecular vibrations, but all of these couplings may essentially be eliminated experimentally by the isotope-isolation technique, which makes the stretching motion involving the isotope-isolated species become a well localized mode, uncoupled from all other modes. As described below, our vibrational calculations also refer to the uncoupled stretching vibrations of isotope-isolated HDO molecules in solution.

IR measurements for an isotope-isolated $LiClO_4$(aq) solution reported by Lindgren et al.[14] using the double-difference method, resulted in an uncoupled O−D stretching vibrational band with a peak maximum at 2530 ($\pm$14) cm^{-1}, i.e., slightly above the bulk water value at 2505 cm^{-1}.[4] Lindgren et al. interpreted this band maximum as coming from all water molecules perturbed by the Li^+ ion, and proposed two dominating contributions to the band: one more low-lying contribution originating from the first-shell water molecules, and one contribution, slightly higher in frequency, originating from those second-shell OH bonds which form hydrogen bonds to the oxygen lone-pair region of a first-shell water and which are thus oriented in an energetically

* Corresponding author. E-mail: kersti@mkem.uu.se.
† "Sts. Cyril and Methodius University".
‡ Uppsala University.

10.1021/jp047395j CCC: $30.25
Published on Web 05/20/2005

unfavorable way with respect to the cation. To make a very rough estimate, let us assume a difference of some 60 cm^{-1} between the maxima of these two (unresolved) peak contributions; this would yield an O−D peak value at ca. 2500 cm^{-1} for the first-shell water molecules. An additional band, a shoulder band observed at approximately 2440 cm^{-1}, was not interpreted as a first-shell contribution in the study by Lindgren et al., in contrast to the isotope-isolated double-difference study of $LiCF_3COO$(aq) by Stangret and Gampe,[15] where careful variable-concentration studies made the authors conclude that it is this band, and not the higher-frequency band discussed by Lindgren et al., which contains the first-shell O−D stretching contributions.

For consistency, and without any loss of generality, we will in the following always discuss OH (and not OD) frequencies. Thus, the corresponding uncoupled experimental ν(OH) value of Stangret and Gampe is 3290 cm^{-1}, using a conversion factor of 1.347 from the experimental correlation curve presented by Berglund et al. (Figure 2 in ref 16), based on IR data for 25 crystalline hydrates. Using the same correlation curve gives a conversion factor of 1.353 to convert the first-shell OD frequency reported by Lindgren et al.; this yields an OH frequency of 3420 cm^{-1}. On the basis of the spread of the experimental points around the fitted conversion curve in ref 16, we judge the uncertainty in the conversion procedure to give rise to uncertainties of ±10 cm^{-1} in the converted OH frequencies. We conclude that the peak maximum of the experimental OH stretching band for the uncoupled ν(OH) frequency for first-shell waters in dilute Li^+(aq) solutions lies somewhere in the range 3290−3420 cm^{-1}, where we are inclined to rely slightly more on the lower-lying value.[17]

Whichever experimental Li^+(aq) value is chosen for reference, we can conclude that the OH oscillator of a first-shell water molecule around Li^+ is about equally much affected by its environment as an average water molecule in pure liquid water; the ν(OH) band in liquid water peaks at approximately 3400 cm^{-1} [4] and is thus downshifted by approximately −310 cm^{-1} with respect to the free HDO(g) value at 3707 cm^{-1}.[18] This is interesting, since the environments are very different. A water molecule in the first hydration shell around Li^+ participates in cation−water interactions not present in the pure liquid, but also the other intermolecular interactions, such as the unfavorable dipolar interactions between water molecules within the first hydration shell (around an ion or around "a central" water molecule), the H-bonded interactions between the first and second hydration shells, and the long-range electrostatic interactions, would be different in liquid water and Li^+(aq). For some of the trivalent cations, the experimental OH frequency downshifts (with respect to the gas-phase value) observed for first-shell water molecules are about three times as large as for Li^+.[15,19]

Also *theoretical* vibrational studies of solvated cations are accompanied by many complications, the most important being (i) how to arrive at a correct structural model for the solution, (ii) how to take temperature effects into account, (iii) how to simultaneously treat *intra*molecular as well as short- and long-range *inter*molecular interactions accurately in the description of the potential energy surface, (iv) how to solve the many-body vibrational problem, and (v) how to take anharmonicity into account. In the present study of Li^+(aq), we have used the following strategies to address these difficulties: (i) we use the molecular geometries generated from a statistical-mechanical computer simulation based on a reasonably good force-field; (ii) the configurational broadening is taken into account by considering different simulation snapshots at 300 K and computing many different OH potential energy curves in a "frozen-field" approach; (iii) the potential energy curves are derived from quantum-mechanical calculations of charge-embedded supermolecules where the probed intramolecular bond and all the most relevant intermolecular interactions are treated at the same level of accuracy; and (iv and v) the multidimensional anharmonic vibrational problem is reduced to a simple-to-solve one-dimensional anharmonic oscillator problem by considering uncoupled HDO molecules, just as was done in the available experiments.

In the present paper we report theoretical *absolute frequencies* as well as *frequency shifts* and no scaling factors have been used. It is not uncommon in the literature to multiply calculated vibrational frequencies with a "magic" scaling factor to improve the agreement between experiment and theory, for example when anharmonicity and electron correlation effects cannot be properly taken into account in the calculations. This can be a practical routine when the calculated frequencies are used as a tool in the assignment of experimentally observed peaks to the proper vibrational modes, for example. For our objectives in the present paper, however, this is an undesirable strategy since the whole purpose of this study is to explore how well our theoretical calculations perform in reproducing *the experimentally observed* OH vibrational frequency at around 3400 cm^{-1} in Li^+(aq), where anharmonicity, electron correlation and solvation-induced effects participate in an intricate interplay, each making a contribution on the order of several hundred reciprocal centimeters.

Our approach of using snapshots from a statistical-mechanical simulation in subsequent ab initio calculations was first presented in the literature over 10 years ago, in a combined "Monte Carlo simulation + supermolecular QM calculations" study of OH vibrational frequencies in liquid water.[20] Those bulk water calculations, performed at the Hartree−Fock and MP2 levels of theory for small charge-embedded supermolecules, gave quite promising results. We recently used the method again, this time to study water in a dilute Al^{3+}(aq) solution.[21] The Al^{3+}(aq) results were not impressive, yielding a B3LYP/6-31G(d,p) gas-to-solution downshift of only 60% of the experimental value. We now believe that the main flaw of the latter study was the quality of the molecular dynamics-generated geometry snapshots.[22] In the present Li^+(aq) study, the two most important differences to the Al^{3+}(aq) study are that (i) the MD simulations have been performed with a newly generated and carefully assessed effective three-body ion−water force field and (ii) the solvent interactions with the monovalent lithium ion are "less demanding" to model than with the trivalent aluminum ion. Future papers will also report the results for Al^{3+}(aq) and other multivalent ions, using our new family of force fields.

In the past decade, there have appeared in the literature a (modest) number of other studies using a similar approach, where bulk solvent or ionic solution properties have been modeled by electronic structure calculations based on statistical-mechanical simulation-derived geometries. A few such examples are the study of the quadrupole coupling constant in liquid water,[23] NMR chemical shifts in isolated water molecules and various supermolecules based on MD-generated water positions,[24−26] and the UV−vis and other spectroscopic calculations for organic molecules in solution by Canuto et al. (see, for example, refs 27 and 28).

Moreover, the Li^+(aq) system has previously been studied by other hybrid approaches in the literature. Car−Parrinello MD

simulations were performed by Lyubartsev et al.[29] for one Li^+ ion and 32 water molecules covering 20 ps at room temperature. From the Fourier transform of the velocity autocorrelation function taken over different types of water molecules, the authors concluded that they could not observe any noticeable differences in the OH stretching bands between hydrated water and bulk water, a conclusion which is in general agreement with experiment. As far as the absolute frequencies are concerned, however, the agreement with experiment was less good, since the Fourier transform of the velocity autocorrelation function taken over all atoms (Figure 6 in ref 29) showed an OH stretching band with a maximum at 3300−3400 cm^{-1}). Considering that the CPMD method gives essentially harmonic frequencies, and that anharmonicity causes a downshift of approximately 200 cm^{-1} in this frequency region, the absolute position of the OH band from these CPMD simulations is thus positioned many hundreds of wavenumbers lower than the experimental values around 3300−3400 cm^{-1}.

Loeffler and Rode[30] and Loeffler et al.[31] recently investigated the hydration structure around the Li^+ ion using the QM/MM-MD method, where the total system is partitioned into a quantum-mechanical region and a region treated by molecular mechanics and both regions are included in the classical MD simulations. The OH stretching vibrations were not discussed in these papers.

The layout of the paper is the following. First we describe the methodological aspects in more detail. In the Results section, the calculated IR shifts will be compared with experiment, and the capabilities of our MD+QM method will be scrutinized. The possible influence of third-shell water molecules on the frequency downshift will be commented on. Moreover, the existence of H-bond correlations in liquids will be discussed.

2. Computational Details

2.1. MD Simulation. A molecular dynamics simulation production run was performed within the NPT (isothermal and isobaric, with a fixed number of particles) ensemble for a Li^+(aq) solution. The temperature was kept at an average of 298K using the extended system method of Nosé and Hoover[32,33] and the pressure was kept at an average of 0 Pa with the method of Hoover.[33] The MD box contained 512 water molecules and one cation, and the counterion charge was implicitly included by the charged-system term.[34] Cubic periodic boundary conditions were used for all two-body interactions and Ewald lattice sums[35] were used for the Coulomb interactions. The average box length during the simulation was approximately 25 Å. The water molecules were kept rigid in the simulation using the RATTLE version[36] of the SHAKE method of constraint dynamics.[37] The velocity version[38] of the Verlet integrator[39] was used.

The force fields used were Berendsen's SPC/E[40] model for the water−water interactions and for the ion−water interactions a newly constructed effective two-body plus three-body potential was used.[41] This ion−water potential is based on ab initio calculations for many hundreds of distorted $Li^+(H_2O)_n$ water clusters with $n = 1$, 4, and 6, and thus includes high-order ion−water many-body effects, but in "an effective way", since the potential expression contains only two-body and three-body terms. The two-body ion−water short-range terms are expressed as sums over ion-O and ion-H pair interactions of the Buckingham type (exponential + inverse 4 and 6 polynomial terms) for all pairs, here taken out to 14.0 Å from the ion. Three-body terms are calculated as sums over water−ion−water triplets (here out to 6.0 Å from the ion) and are expressed as functions of the cosine of the oxygen-ion−oxygen angle as well as of the two ion−oxygen distances involved. The coefficients in these analytical expressions were derived by least-squares fitting to the ab initio calculated interaction energies for the many hundreds of distorted clusters (see above) at the counterpoise-corrected MP2/TZV++(d,p) level (see ref 41 for details).

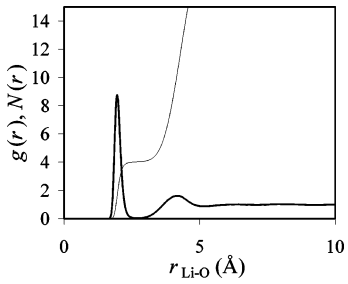

Figure 1. Li−O radial distribution function and the running coordination number calculated from the MD simulation.

The equilibration procedure was rather elaborate and was described in detail in ref 41; it was carefully checked that equilibrium had been reached. The equilibration run was approximately 30 ps long. The simulation run was 900 ps long with a time step of 1.5 fs. The resulting Li−O radial distribution function and the running coordination number are shown in Figure 1. The number of water molecules in the first hydration shell is 4.0.

2.2. Electronic Structure Calculations Applied to the MD-Generated Geometries. Quantum-mechanical calculations were subsequently carried out for 50 water molecules (100 O−H oscillators) from the *first hydration shell* around Li^+ in order to obtain the uncoupled anharmonic O−H stretching frequencies. These water molecules were selected from a series of 12 snapshots from the MD simulations, chosen 0.9 ps apart in time, providing a sufficiently large time interval between the selected configurations, so that they could be considered mutually uncorrelated. For each first-shell O−H oscillator, a series of point-charge-embedded *supermolecular* cluster single-point energy calculations were carried out to obtain the *anharmonic* O−H stretching potential. These clusters consisted of the central Li^+ cation, all four first-shell water molecules (five in very few cases), plus "the relevant" second hydration-shell water molecules; the remaining part of the ionic solution, namely the "bath" of bulk water molecules, was treated as point-charge molecules. A second-shell neighbor of the vibrating first-shell O−H oscillator was included in the supermolecular cluster if the MD-generated H···O distance between the vibrating H and the neighboring water molecule was smaller that 2.5 Å. Thus, the supermolecules explicitly described by ab initio or DFT single-determinant wave functions were of the form $Li(H_2O)_x$-$(H_2O)_y^+$, where $x = 4$ (or 5 for a few cases) and $y = 2$ (or 3 for a few cases).

Two sets of 10 oscillators (out of the 100) were selected as *test sets*, for which different methodological aspects were tested. So, for example, it was confirmed by a series of calculations for one of these test sets that explicit inclusion of *all* the (approximately 15) second hydration-shell water molecules in the supermolecular calculations has an essentially negligible effect on the O−H frequencies in the first hydration shell (while increasing the computational cost significantly). Test calculations were also performed where a part of the third shell was included in the supermolecular cluster instead of as point-charge molecules; more details are given in section 2.3.

To generate the O−H stretching potentials for the point-charge embedded supermolecular systems, Hartree−Fock (HF)

and density functional theory (DFT) calculations were employed for all selected 100 oscillators. The standard Pople-type 6-31G-(d,p) basis set was employed for the orbital expansion, solving the HF or the Kohn−Sham (KS) SCF equations iteratively. All quantum-chemical calculations were performed with the Gaussian98 program.[42]

Within the DFT approach, the combination of Becke's three-parameter adiabatic connection exchange functional (B3,[43]) with the Lee−Yang−Parr correlation functional (LYP[44]) was employed. Test calculations were performed for one of the test sets of 10 oscillators also employing the combination of the Perdew−Wang 1991 exchange functional as modified by Adamo and Barone (mPW1[45]) with the Perdew and Wang's 1991 gradient-corrected correlation functional (PW91[46]—mPW1PW91), since these functionals were constructed with the main aim of improving the well-known deficiency in the long-range behavior of DFT functionals, which is of particular importance when studying intermolecular interactions. The effect of this change of functionals will be commented on in the Discussion part. The "fine" (75, 302) grid was used for numerical integration in all DFT calculations (75 radial and 302 angular integration points). To test the reliability of the previously mentioned theoretical levels, MP2 calculations were also carried out for the same test set, with the same basis set.

2.3. The Long-Range Effects. As already mentioned, the long-range electrostatic influence from all the water molecules not explicitly included in the quantum-mechanical cluster was accounted for by immersing the supermolecule in a "bath" of point-charges, placed at the MD-generated oxygen and hydrogen atomic positions. The bulk solvent water molecules contained within spheres of successively larger radii surrounding the central Li^+ ion were included as point-charges until a sufficient convergence of the uncoupled O−H stretching frequencies of the 10 test oscillators was achieved (within 4−5 cm^{-1}). This convergence was achieved for a cutoff radius of 11 Å, which was the final cutoff applied in all the subsequent calculations. In this way, about 100 bulk water molecules were included as "point-charge water molecules" in the quantum-mechanical energy calculations. The values of the point charges chosen to model the "permanent + average induced" dipole moment of the bulk water molecules were −0.80 *e* for O and +0.40 *e* for H. These charges yield a water dipole moment of 2.22 D, which is in a good agreement with (although on the low side of) the literature estimates of the water dipole moment in liquid water and ice.[47] Test calculations with the point-charge values enhanced by 10% were carried out for several oscillators as well, and the effect on the calculated stretching frequencies was found to be 10 cm^{-1} or smaller.

2.4. Calculation of Anharmonic Uncoupled O−H Vibrational Frequencies and the Dipole Moment Derivatives. The experimentally reported frequencies[14,15] contain significant anharmonic contributions. The calculation of the uncoupled anharmonic O−H stretching frequencies for the 100 O−H oscillators considered proceeded in the following manner. To obtain the vibrational potential for a particular OH oscillator (the $V = f(r_{OH})$ function), a series of 20 pointwise HF, DFT or MP2 energy calculations were performed for each O−H oscillator, varying the O−H distances from 0.90 to 1.20 Å.

The nuclear displacements corresponding to the uncoupled O−H stretching vibration were generated so as to keep the center-of-mass of the vibrating molecule, as well as the water angle, fixed, thereby mimicking as closely as possible the uncoupled OH normal stretching mode of a HDO molecule. The obtained energies were least-squares fitted to a fifth-order polynomial in Δr_{OH} ($\Delta r = r - r_e$): $V = V_0 + k_2\Delta r^2 + k_3\Delta r^3 + k_4\Delta r^4 + k_5\Delta r^5$. The resulting potential energy functions were subsequently cut after fourth order and transformed into Simons−Parr−Finlan (SPF) type coordinates $\rho = 1 - r_{OH,e}/r_{OH}$[40,41] ($r_{OH,e}$ being the equilibrium, i.e., the lowest-energy, value). The one-dimensional vibrational Schrödinger equation was solved variationally using 15 harmonic oscillator eigenfunctions as a basis. Superiority of the SPF-type coordinates over the "ordinary" bond stretch ones when a variational solution of the vibrational Schrödinger equation is sought has been well established, as they allow for a faster convergence (for the number of basis functions used) and a greatly extended region of convergence.[48,49] The fundamental *anharmonic* O−H stretching frequency was computed from the energy difference between the ground and first excited vibrational states.

When this method was applied to the gas-phase water molecule (i.e., with the angle and the distance of the nonvibrating OH bond fixed at their experimental equilibrium values), the fundamental uncoupled anharmonic O−H stretching frequencies obtained using the 6-31G(d,p) basis set were 4017 cm^{-1} at the HF level of theory, 3684 cm^{-1} at the B3LYP level, 3771 cm^{-1} at the mPW1PW91 level and 3786 cm^{-1} at the MP2 level. The experimental value is 3707 cm^{-1}.[18] Thus, at the B3LYP/6-31G(d,p) level, which is the method used for the majority of the results given in the present paper, the absolute OH frequency for the free water molecule differs by less than 25 cm^{-1} from the experimental value.

The calculated uncoupled *anharmonic* O−H stretching frequencies for the MD-generated Li^+(aq) solution configurations were used to generate *density-of-states histograms*, which are a good approximation to experimentally obtained Raman bands. However, for a comparison with the IR bands to be possible, it is necessary to take into account the transition dipole moment variation with the ν(O−H) frequency. In the present study, the density-of-states histograms were converted to IR intensity-weighted histograms by means of the transition dipole moment function $|d\vec{\mu}/dr|^2$.[50] The transition dipole moment function was calculated for each oscillator at r_e from the expression:

$$\left(\frac{d\vec{\mu}}{dr_{OH}}\right)_{r_{OH,e}}^2 = \left(\frac{d\mu_x}{dr_{OH}}\right)_{r_{OH,e}}^2 + \left(\frac{d\mu_y}{dr_{OH}}\right)_{r_{OH,e}}^2 + \left(\frac{d\mu_z}{dr_{OH}}\right)_{r_{OH,e}}^2 \quad (1)$$

Each of the derivatives on the right-hand side of eq 1 was computed by a fourth-order polynomial interpolation of the corresponding $\mu_i(r_{OH})$ function and subsequent differentiation at $r_{OH,e}$. Newton's first interpolation formulas were used for both the fourth-order polynomial interpolation and the numerical differentiation.[51]

3. Results and Discussion

3.1. Absolute OH Frequencies and Frequency Shifts. As mentioned in the Introduction, the experimentally measured downshift of the uncoupled O−H stretching vibrational frequency of water molecules in the first hydration shell around Li^+ lies in the approximate range from −290 to −420 cm^{-1} with respect to the gas-phase value. The theoretical density-of-states (DOS) histograms for the OH stretching frequency distributions computed at the HF and B3LYP levels of theory for the charge-embedded $Li(H_2O)_x(H_2O)_y^+$ clusters are presented in Figures 2a and 3a. In Table 1, the average O−H stretching frequencies as well as the frequency shifts with respect to the free water molecule are given. Note that most of the absolute frequencies and frequency shifts discussed for the Li^+(aq) solution in the following have been rounded off to the nearest

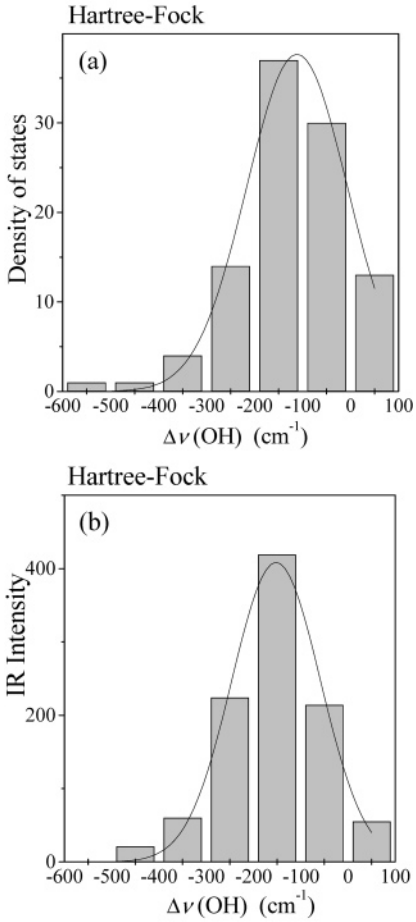

Figure 2. (a) Density-of-states diagram for the HF frequencies for the 100 selected anharmonic OH oscillators belonging to water molecules in the first hydration shell of the Li^+ ion. Here and in the following figures, the frequency shift will always refer to the anharmonic frequency of the uncoupled OH vibration of the optimized gas-phase HDO molecule at the computational level discussed. (b) IR intensity-weighted histogram.

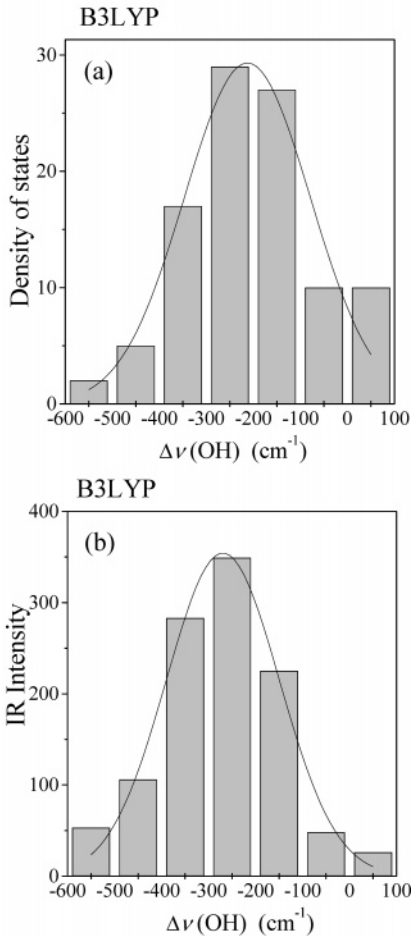

Figure 3. (a) Density-of-states diagram for the B3LYP frequencies for the 100 selected anharmonic OH oscillators belonging to water molecules in the first hydration shell of the Li^+ ion. (b) IR intensity-weighted histogram.

5 cm^{-1} for visibility; differences as small as a few wavenumbers are insignificant in the present context. The average frequency downshifts calculated directly from the DOS distributions are -115 and -205 cm^{-1} at the HF and B3LYP levels, respectively. The spread in the calculated OH stretching frequencies is substantial and arises from the variety of geometrical configurations present. The full widths at half-maximum intensity (the fwhh values), calculated from a Gaussian function fit to the DOS histograms are approximately 250 and 315 cm^{-1} at the HF and B3LYP levels, respectively.

Figures 2b and 3b present the IR intensity histograms at the HF and B3LYP levels.

At the HF level, the transition dipole moment function values used in the conversion from DOS histograms to IR intensities lie in the range from 1.8 $D^2/Å^2$ for the most loosely bound first-shell water molecules to 24.5 $D^2/Å^2$ for the most strongly bound ones investigated in this study (the value for the free water at this level of theory is 0.81 $D^2/Å^2$). At the B3LYP level, the 100 oscillators lie in the range 1.3 $D^2/Å^2 < |d\vec{\mu}/dr|^2 < 28.6$ $D^2/Å^2$ (free water value: 0.89 $D^2/Å^2$). These results are consistent with the experimental data, both qualitatively and quantitatively, as it is well-known that the IR intensity of the stretching vibration of an O−H hydrogen-bond donor increases by a factor of more than 10 upon increase of the hydrogen-bond strength in the frequency range considered here.[52] Calculated $|d\vec{\mu}/dr|^2$ values at the B3LYP level are plotted against the ν(OH) values in Figure 4.

Upon transformation of the DOS histograms to the IR intensity histograms by means of the transition dipole moment function $|d\vec{\mu}/dr|^2$, the average frequency downshifts become -155 and -275 cm^{-1} at the HF and B3LYP levels, i.e. considerably larger in magnitude than the DOS values. We conclude so far that the IR intensity-weighted band for the charge-embedded $Li(H_2O)_x(H_2O)_y^+$ clusters gives a peak maximum at 3410 cm^{-1} at the B3LYP level, and a frequency shift of -275 cm^{-1}; both are in reasonable agreement with experiment. The fwhh values calculated from a Gaussian function fit to the IR intensity histograms are approximately 220 and 280 cm^{-1} at the HF and B3LYP levels, respectively, and thus similar to (only slightly smaller than) the widths of the DOS histograms; all are broader than the experimental bandwidth, however.

In hydrogen-bonded media, long-range cooperative effects are important and when such condensed phases are modeled by finite-cluster ab initio quantum-chemical methods, the effects of the medium surrounding the QM cluster can at least partially be taken into account by using some less sophisticated treatment such as a set of point charges (as in our case), or by a lower-level wave function (e.g., as in the case of the ONIOM-type approach[53,54]). Regardless of approach, at the border of the wave function region, the consistent description of the long-range cooperative effects is truncated and potential problems arise. Moreover, any unshielded point charges too close to the wave

TABLE 1: Calculated Average OH Frequencies and Frequency Shifts (in cm^{-1}) for Water Molecules in the First Hydration Shell of a Solvated Li^+ Ion[d]

	Hartree−Fock		B3LYP		experiment[c]	
type of frequency	⟨ν⟩	⟨Δν⟩	⟨ν⟩	⟨Δν⟩	⟨ν⟩	⟨Δν⟩
HDO(g)[a]	4015		3685		3707	
first shell around Li^+						
DOS band (1st + 2nd shells)	3900	−115	3480	−205		
IR band (1st + 2nd shells)	3860	−155	3410	−275		
IR band (1st + 2nd + 3rd shells)[b]	3845	−170	3380	−305	3420, 3290	−290, −420

[a] One frequency value, i.e. no average. [b] Estimated downshift based on calculations for the test set described in the text. [c] The gas-phase value is taken from ref 18 and the aqueous solution values are from ref 14 (3420 cm^{-1}) and ref 15 (3290 cm^{-1}), after conversion using the empirical ν(OH)/ν(OD) curve from ref 16 (see text). [d] All frequencies are anharmonic and the calculations used the 6-31G(*d,p*) basis set. Note that all frequency values have been rounded off to the closest 5 cm^{-1} for increased visibility.

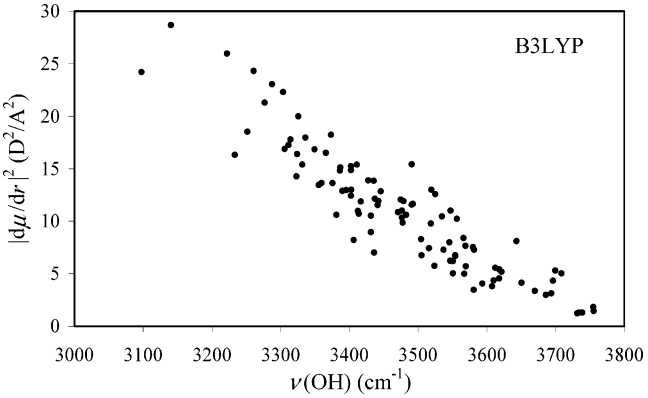

Figure 4. Instantaneous transition dipole moment function vs instantaneous OH stretching frequency for the 100 OH oscillators at the B3LYP level.

function region are likely to corrupt the electron density distribution at the border. Last, but not least important: an artificial buildup of charges takes place at the "edges" of the quantum-mechanical cluster, leading to the generation of an artificial electrostatic field over the supermolecule,[20,55] and an upshift of the calculated OH stretching potential. This phenomenon was observed already in the MC + QM liquid water paper,[20] where pentamer clusters yielded an infrared OH stretching band which was approximately 50 cm^{-1} too little downshifted from the gas-phase value compared to experiment. This effect could be remedied in two different ways, either by expanding the supermolecular cluster to include some outer-shell neighbors of the OH oscillators, or by applying a "field-correction" procedure, which basically consisted of applying a field of the same magnitude but opposite direction as the artificially generated field. In the present paper we attempt to expand the cluster.

Thus, calculations for one of the sets of 10 test oscillators were carried out using (charge-embedded) *extended* supermolecular clusters which explicitly included also part of the third hydration shell in the wave function description. In these cases, a third-shell water molecule was included explicitly in the wave function description if any of the H(second shell)···O(third shell) distances involving the already selected explicit second-shell water molecules was smaller than 2.5 Å. The supermolecules were of the form $Li(H_2O)_x(H_2O)_y(H_2O)_z^+$, where $x = 4$ or 5, $y = 2$ or 3, and $z = 4$ or 5, for most cases. An additional downshift of approximately −20 cm^{-1} at the HF level and approximately −30 cm^{-1} at the B3LYP level was obtained, averaged over the 10 oscillators. The variation of this additional downshift was rather large between the different oscillators, but the value was always negative or very close to zero. Even in the case of these larger clusters, artificial fringe effects still remain, such as the buildup of charges at the border, but these effects are significantly smaller than in the case of the smaller clusters.

To summarize: after inclusion of the third-shell correction, the average calculated IR frequency downshift for the uncoupled, anharmonic OH stretching vibration in the first hydration shell around Li^+ is approximately −305 cm^{-1} at the B3LYP level and thus falls within the interval of the two available experiments, and close to the value given by Lindgren et al.[14] (cf. Table 1).

3.2. Discussion of Errors. Our calculated first hydration-shell $\Delta\nu$(OH) value is −305 cm^{-1}, and, as mentioned in the Introduction, the very careful experimental procedure described in ref 15 may suggest their value ($\Delta\nu$(OH) ≈ −420 cm^{-1}) to be slightly more reliable than the value given by Lindgren et al.[14] ($\Delta\nu$(OH) ≈ −290 cm^{-1}). In this section, we therefore make a brief analysis of possible errors in our calculated frequencies.

First of all, there is an inherent inaccuracy in any *MD-generated geometries*, due to the inexactness of the interaction potentials. The geometries used in this paper are obtained from an effective "pair + three-body" potential for the ion−water interaction in combination with an effective pair potential for water. Details of the potential will affect the resulting ion−water coordination geometries. Thus, for example, using a polarizable water model in combination with an effective "polarizable ion−water" model was found to change the ion···first-shell···second-shell structure, for instance by a straightening of the ion···oxygen···oxygen angle.[56] This effect may have a non-negligible impact on the calculated frequencies.

Second, we will address the question of *how representative the selected oscillators are*. For the full analysis, 100 oscillators were selected from different MD dumps chosen distant enough in time to try to avoid any correlation between them. As for the 10 "test oscillators" they were selected in two different ways: (i) 10 first-shell oscillators from one particular dump; (ii) 10 randomly chosen first-shell oscillators spanning the whole range of the 12 MD dumps. When the test oscillators were used for estimating the additional frequency shift induced by explicit inclusion of the third hydration shell into the supermolecular calculations, the first sampling scheme led to an additional average downshift of about 30 cm^{-1} at the B3LYP level, the second set to 40 cm^{-1}. This (modest) discrepancy demonstrates that some bias may exist in our selection of the 100 oscillators, but the bias appears to be small.

A third possible source of error is the *quantum-mechanical (QM) methodology chosen* for the supermolecule description. An appropriate QM methodology should here be able to describe properly both the intra- and the intermolecular bonding situations. It so happens that the B3LYP/6-31G(d,p) level excellently describes the O−H stretching potential for the free water molecule. However, the intermolecular interaction is not equally well described. For instance, DFT studies at various levels have

been found to overestimate the anharmonic vibrational X−H frequency shift for some small optimized hydrogen-bonded dimers.[57] The standard explanation for this finding is the inadequacy of the currently available exchange-correlation functionals to describe weak intermolecular interactions, i.e., their inappropriate description of the intermolecular region, leading to an overestimation of the hydrogen-bond strength and a too short intermolecular hydrogen-bond distance. Thus, the DFT functionals in current use generally vanish too quickly to zero as the intermolecular distance increases and this leads to wrong Kohn−Sham solutions for the virtual states, the exchange-correlation functionals being severely too shallow.

In the present study we have used MD-generated cluster geometries, not the DFT-generated ones (i.e., not the minima located on the DFT PESs). Thus, the previously mentioned argument against the DFT-derived intermolecular potential energy curve giving too large downshifts should not necessarily be expected to cause a problem in the present case. And indeed, our first hydration-shell in Li^+(aq) does not display a too large gas-to-liquid OH frequency shift compared to experiment, but rather too small a shift, at least compared to ref 15. The discrepancy between experiment and calculation that we observe could still possibly be attributed to the inadequacy of the B3-LYP combination of functionals in describing the intermolecular region. However, we also performed MP2 calculations for one of the 10-oscillator test-set, and the result was not very different from the B3LYP result; the average gas-to-liquid downshift at the MP2 level was ∼15 cm^{-1} smaller than at the B3LYP level. Results using the mPW1PW91 combination of functionals (which was constructed with the main aim of improving the previously mentioned deficiency of the DFT exchange and correlations functionals[37,38] in the low-density high-gradient regions, i.e., in the region of *intermolecular bonding*) were insignificantly different from the B3LYP ones.

Yet another potential source of error—*the exact choice of the point-charge values used in describing the "bath" of bulk water molecules*—may almost certainly be ruled out as a source of significant error, as we have found that the anharmonic OH stretching frequencies of the first-shell water molecules are not significantly sensitive to variations of these parameters (see section 2.3).

All in all, we find no obvious sources of error in our computational strategy, and we conclude that our computational result lies closest to the experimental result of ref 14.

3.3. "In-Liquid" Correlations for ν(OH) vs R(O···O) or R(H···O). For many hydrogen-bonded systems, studied both theoretically and experimentally, the intramolecular OH stretching frequencies have been found to correlate with various intermolecular geometrical parameters that are often used as measures of the intermolecular interaction strength. Two such geometrical parameters are the O···O and H···O hydrogen-bond distances. For crystalline hydrates, experimental correlation curves[58] constructed between IR- or Raman-measured vibrational frequencies and neutron-diffraction-determined O···O and H···O hydrogen-bond distances display robust correlations. The modest scatter in those plots is caused by the different crystalline geometries and neighbor-types for the structures contributing to the plot.

Even though the correlation thus appears to be very good for the crystalline hydrates, it is not immediately obvious that it will be equally good for the Li^+(aq) liquid. The crystalline correlation curves refer to different compounds at their equilibrium structures and it is not obvious that the same correlations should be valid *at each instant in time (snapshot) in a liquid*.

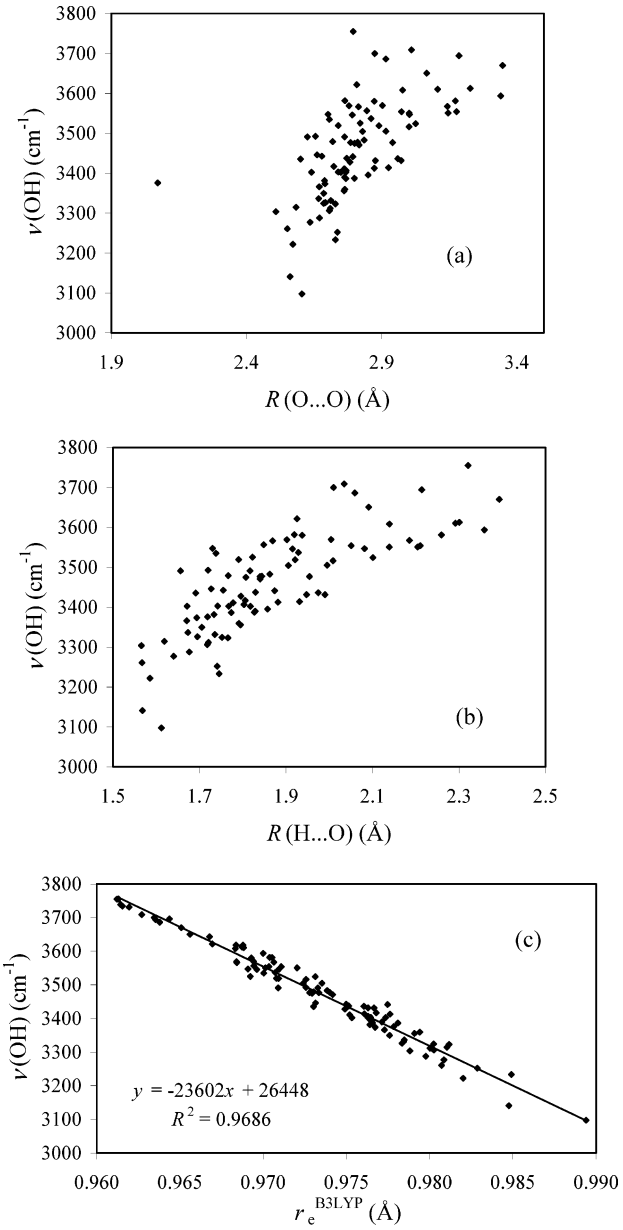

Figure 5. Correlation curves between *instantaneous* "in-solution" values of various quantities often discussed in hydrogen-bond contexts. All graphs refer to the "MD+B3LYP"-generated quantities. (a) Instantaneous OH stretching frequency vs instantaneous O···O distance. (b) Instantaneous OH stretching frequency vs instantaneous H···O distance. (c) Instantaneous OH stretching frequency vs instantaneous equilibrium OH distance.

Figures 5a and b present our calculated plots of ν(OH) vs R(O···O) and R(H···O) at the B3LYP level in the Li^+(aq) solution. The existence of a correlation is evident in both cases, although the spread around the perfect-correlation line is about 50% larger in the liquid than for the crystalline structures mentioned above, because many much more distorted geometries are sampled in the liquid (see also the work of Möller et al.[59] for a discussion of the correlation between calculated instantaneous ν(OH) vs R(O···O) values in liquid water). The spread is smaller in the ν(OH) vs R(H···O) plot than in the ν(OH) vs R(O···O) plot, which is somewhat expected since the H···O distance is a better measure of the H-bond strength than the O···O distance (again, due to the variety of possible H-bond geometries which are represented by a given O···O distance).

3.4. "In-Liquid" Correlation between ν(OH) and r_e(OH). The OH stretching vibrational frequency and the *intra*molecular

TABLE 2: Calculated Average r_e(OH) Values and Δr_e(OH) Gas-to-solution Elongations (in Å) for Water Molecules in the First Hydration Shell of a Solvated Li^+ Ion. The Value for the Isolated HDO Molecule Is Also Given

	Hartree−Fock		B3LYP	
system	$\langle r_e(OH)\rangle$, Å	$\langle \Delta r_e(OH)\rangle$, Å	$\langle r_e(OH)\rangle$, Å	$\langle \Delta r_e(OH)\rangle$, Å
free HDO	0.944		0.965	
first shell around Li^+	0.948	+0.004	0.973	+0.008

equilibrium OH bond distance are both indicators of the overall strength of the *inter*molecular interactions in which the water molecule participates. In the case of crystalline hydrates studied by neutron diffraction, it has been found that the R(O···O) length of the hydrogen bonds donated by the water molecules usually lie in the range 2.6−3.0 Å and that the water O−H bond is elongated by up to 0.02 Å[60] compared to the gas-phase value. In our present computational investigation, the elongation of r_e(OH) is 0.004 Å at the HF level of theory (cf. Table 2) and 0.008 Å at the B3LYP level, and is caused by the Li^+−water interactions, by the hydrogen bonds donated to the second-shell water molecules and also by occasional H-bonds donated from the second to the first shell water O atoms.[56]

Experimental correlation curves of the form "ν(OH) vs r_e(OH)" are difficult to construct directly from the experimental data because the systematic error inherent in intramolecular OH or OD distances determined by neutron diffraction is on the order of 0.02 Å; this is mainly a consequence of a mismatch between the vibrational model used in the crystallographic least-squares refinement, and reality. Nevertheless, La Placa et al. [61] published such an *experimental* correlation curve, making use of a few crystal structures which spanned a large range in intermolecular interactions, from weak to strong hydrogen bonds. Their (ν(OD), r(OD)) data points were found to lie on an approximately straight line. A *theoretical* correlation curve constructed from ab initio calculations for several crystalline hydrates also showed an excellent correlation between ν(OH) and r_e(OH) with a slope of $-24\,500$ cm^{-1}/Å.[62]

In Figure 5c, a plot of the instantaneous uncoupled OH frequencies vs r_e(OH) at the B3LYP level of theory for Li^+(aq) is given. The ν(OH) vs r_e(OH) dependence is seen to be quite linear indeed. Least-squares fits give slopes of $-23\,602$ cm^{-1}/Å at the B3LYP level ($R^2 = 0.9686$), and $-24\,102$ cm^{-1}/Å at the HF level ($R^2 = 0.8908$) (not shown here), the correlation being somewhat better at the B3LYP level. The values of the slopes obtained here are rather similar to those reported for the Al^{3+}(aq)[21] and pure liquid water[20] simulations in our previous papers and to the crystalline hydrate values quoted above.

The spread around the least-squares line is some 25 cm^{-1} at the B3LYP level, which is mainly due to the different environments for the different vibrating water molecules (straight and bent H-bonds, different degree of water tilting toward the cation, etc.). It is seen, however, that these geometrical parameters do not destroy the robust correlation between OH distance and OH frequency. This is in fact contrary to what we found for the correlation between the instantaneous values of the transition dipole moment function and the OH frequency in Figure 4; the latter correlation is seen to be less robust and appears to be more sensitive to the explicit instantaneous geometries.

4. Conclusions

A hybrid "MD + QM" approach was employed to calculate the infrared peak position of the uncoupled OH stretching band for the first hydration-shell water molecules in a dilute Li^+(aq) solution. The average frequency at the B3LYP level of theory, including second- and third-shell effects as well as anharmonicity, falls at approximately 3380 cm^{-1} (experimental values in the range 3290 [15] to 3420 cm^{-1} [14]), and the calculated downshift is approximately -305 cm^{-1} (experimental values in the range -290 to -420 cm^{-1}). Thus, both the absolute OH frequency value and the frequency shift agree very well with ref 15 and reasonably well with ref 16.

The transition dipole moment function varies by a factor of 20 over the frequency region at the B3LYP level.

Various "instantaneous, in-liquid" correlation curves were calculated between traditional H-bond-characterizing quantities such as the intermolecular R(O···O) and R(H···O) distances, the intramolecular OH bond, the OH vibrational frequency and the IR intensity. Some of these correlations are strong and persist also for the rather distorted instantaneous geometries in the liquid; others are less so.

Acknowledgment. The authors acknowledge the support of The Swedish Research Council (VR) and Ångpanneföreningens Forskningsstiftelse. Valuable discussions with Professor Jan Lindgren are also gratefully acknowledged.

References and Notes

(1) Ohtaki, H.; Radnai, T. *Chem. Rev.* **1993**, *93*, 1157.
(2) Richens, D. T. *The Chemistry of Aqua Ions*; Wiley: Chichester, England, 1997.
(3) Luck, W. A. P. In *Water, A Comprehensive Treatise*; Franks, F., Ed.; Plenum: New York, 1973; Vol. 2.
(4) Verrall, R. E. In *Water, A Comprehensive Treatise*; Franks, F., Ed.; Plenum: New York, 1973; Vol. 3.
(5) Lilley, T. H. In *Water, A Comprehensive Treatise*; Franks, F., Ed.; Plenum: New York, 1973; Vol. 3.
(6) Conway, B. E. *Ionic Hydration in Chemistry and Biophysics*; Elsevier: Amsterdam, 1981; Chapters 7 and 8.
(7) Zundel, G.; Fritsch, J. In *The Chemical Physics of Solvation*; Dogonadze, R. R., Kálmán, E., Kornyshev, A. A., Ulstrup, J., Eds.; Elsevier: Amsterdam, 1986; Part B, Chapters 2 and 3.
(8) Eriksson, A.; Kristiansson, O. *J. Mol. Struct.* **1984**, *114*, 455.
(9) Kristiansson, O.; Eriksson, A.; Lindgren, J. *Acta Chem. Scand.* **1984**, *38*, 609.
(10) Kristiansson, O.; Lindgren, J.; de Villepin, J. *J. Phys. Chem.* **1988**, *92*, 2680.
(11) Waldron, R. D. *J. Chem. Phys.* **1957**, *26*, 809.
(12) Horning, D. F. *J. Chem. Phys.* **1964**, *40*, 3119.
(13) Falk, M.; Ford, T. A. *Can. J. Chem.* **1966**, *44*, 1699.
(14) Lindgren, J.; Hermansson, K.; Wójcik, M. J. *J. Phys. Chem.* **1993**, *97*, 5254.
(15) Stangret, J.; Gampe, T. *J. Phys. Chem.* **2002**, *106*, 5393.
(16) Berglund, B.; Lindgren, J.; Tegenfeldt, J. *J. Mol. Struct.* **1978**, *43*, 169.
(17) Lindgren, J. Private communication.
(18) Benedict, W. S.; Gailar, N.; Plyler, E. K. *J. Chem. Phys.* **1956**, *24*, 1139.
(19) Bergström, P.-Å.; Lindgren, J.; Read, M.; Sandström, M. *J. Phys. Chem.* **1991**, *95*, 7650.
(20) Hermansson, K.; Knuts, S.; Lindgren, J. *J. Chem. Phys.* **1991**, *95*, 7486.
(21) Pejov, Lj.; Hermansson, K. *J. Mol. Liq.* **2002**, *98−99*, 367.
(22) Lauenstein, A.; Hermansson, K.; Lindgren, J.; Probst, M.; Bopp, P. A. *Int. J. Quantum Chem.* **2000**, *80*, 892.
(23) Eggenberger, R.; Gerber, S.; Huber, H.; Searles, D.; Welker, M. *Mol. Phys.* **1993**, *80*, 1177.
(24) Chestnut, D. B.; Rusiloski, B. E. *J. Mol. Struct.* **1994**, *314*, 19.
(25) Malkin, V. G.; Malkina, O. L.; Steinebrunner, G.; Huber, H. *Chem.−Eur. J.* **1996**, *2*, 452.
(26) Nymand, T. M.; Åstrand, P.-O.; Mikkelsen, K. V. *J. Phys. Chem. B* **1997**, *101*, 4105.
(27) Coutinho, K.; Canuto, S. *Adv. Quantum Chem.* **1997**, *28*, 89.
(28) Canuto, S.; Coutinho, K. *Chem. Phys. Lett.* **1998**, *313*, 235.
(29) Lyubartsev, A. P.; Laasonen, K.; Laaksonen, A. *J. Chem. Phys.* **2001**, *114*, 3120.
(30) Loeffler, H. H.; Rode, B. M. *J. Chem. Phys.* **2002**, *117*, 110.
(31) Loeffler, H. H.; Mohammed, A. M.; Inada, Y.; Funahashi, S. *Chem. Phys. Lett.* **2003**, *379*, 452.
(32) Nosé, S. *Mol. Phys.* **1984**, *52*, 255.
(33) Hoover, W. G. *Phys. Rev. A* **1985**, *31*, 1695.

(34) Hummer, G.; Pratt, L. R.; Garcia, A. E. *J. Phys. Chem.* **1996**, *100*, 1206.
(35) Allen, M. P.; Tildesley, D. J. *Computer Simulation of Liquids*; Clarendon: Oxford, England, 1987.
(36) Andersen, H. C. *J. Comput. Phys.* **1983**, *52*, 24.
(37) Ryckaert, J. P.; Ciccotti, G.; Berendsen, H. J. C. *J. Comput. Phys.* **1977**, *23*, 327.
(38) Swope, W. C.; Andersen, H. C.; Berens, P. H.; Wilson, K. R. *J. Chem. Phys.* **1982**, *76*, 637.
(39) Verlet, L. *Phys. Rev.* **1967**, *159*, 98.
(40) Berendsen, H. J. C.; Grigera, J. R.; Straatsma, T. P. *J. Phys. Chem.* **1987**, *91*, 6269.
(41) Spångberg, D.; Hermansson, K. *J. Chem. Phys.* **2003**, *119*, 313.
(42) Frisch, M. J.; et al. *Gaussian 98*, Revision A.1. Gaussian, Inc.: Pittsburgh, PA, 1998.
(43) Becke, A. D. *Phys. Rev. A* **1988**, *38*, 3098.
(44) Lee, C.; Yang, W.; Parr, R. G. *Phys. Rev. B* **1988**, *37*, 785.
(45) Adamo, C.; Barone, V. *J. Chem. Phys.* **1998**, *108*, 664.
(46) Perdew, J. P.; Burke, K.; Wang, Y. *Phys. Rev. B* **1996**, *54*, 16533.
(47) Spackman, M. A. *Chem. Rev.* **1992**, *92*, 1769.
(48) Simons, G.; Parr, R. G.; Finlan, J. M. *J. Chem. Phys.* **1973**, *59*, 3229.
(49) Carney, D. G.; Curtiss, L. A.; Langhoff, S. R. *J. Mol. Spectrosc.* **1976**, *61*, 371.
(50) Herzberg, G. *Spectra of Diatomic Molecules*; van Nostrand-Reinhold: New York, 1950.
(51) Wylie, C. R.; Barrett, L. C. *Advanced Engineering Mathematics*; McGraw-Hill: New York, 1995.
(52) Glew, D. N.; Rath, N. S. *Can. J. Chem.* **1971**, *49*, 838.
(53) Humbel, S.; Sieber, S.; Morokuma, K. *J. Chem. Phys.* **1996**, *105*, 1959.
(54) Maseras, F.; Morokuma, K. *J. Comput. Chem.* **1995**, *16*, 1170.
(55) Hermansson, K.; Alfredsson, M. *J. Chem. Phys.* **1999**, *111*, 1993.
(56) Spångberg, D.; Hermansson, K. *J. Chem. Phys.* **2004**, *120*, 4829.
(57) Silvi, B.; Wieczorek, R.; Latajka, Z.; Alikhani, M. E.; Dkhissi, A.; Bouteiller, Y. *J. Chem. Phys.* **1999**, *111*, 6671.
(58) Berglund, B.; Lindgren, J.; Tegenfeldt, J. *J. Mol. Struct.* **1978**, *43*, 179.
(59) Möller, K. B.; Rey, R.; Hynes, J. T. *J. Phys. Chem. A* **2004**, *108*, 1275.
(60) Olovsson, I.; Jönsson, P.-G. In *The Hydrogen Bond-Recent Developments in Theory and Experiments*; Schuster, P., Zundel, G., Sandorfy, C., Eds.; North-Holland: Amsterdam, 1976; Vol. 2.
(61) La Placa, S. J.; Hamilton, W. C.; Kamb, B.; Praksh, A. *J. Chem. Phys.* **1973**, *58*, 567.
(62) Ojamäe, L.; Hermansson, K. *J. Chem. Phys.* **1992**, *96*, 9035.